Journal of Nuclear Medicine, published on December 2, 2022 as doi:10.2967/jnumed.122.264586

^{64}Cu Treatment Planning and ^{67}Cu Therapy with Radiolabelled SARTATE ([^{64}Cu/^{67}Cu]MeCOSAR-Octreotate) in Subjects with Unresectable Multifocal Meningioma – Initial Results for Human Imaging, Safety, Biodistribution and Radiation Dosimetry

Dale L Bailey[1-3], Kathy P Willowson[1,4], Matthew Harris[5], Colin Biggin[5], Alireza Aslani[1,2], Nigel A Lengkeek[6], Jon Stoner[7], M Enid Eslick[1], Harry Marquis[3,4], Michelle Parker[5], Paul J Roach[1,2] and Geoffrey P Schembri[1,2]

[1]Department of Nuclear Medicine, Royal North Shore Hospital, Sydney, Australia

[2]Faculty of Medicine & Health, University of Sydney, Sydney, Australia

[3]Sydney Vital Translational Cancer Research Centre, Sydney, Australia

[4]Institute of Medical Physics, University of Sydney, Sydney, Australia

[5]Clarity Pharmaceuticals, Sydney, Australia

[6]ANSTO Biosciences, Sydney, Australia

[7]Idaho Accelerator Center, Idaho State University, Pocatello, Idaho, USA

Email: dale.bailey@sydney.edu.au

Contact address for all correspondence and first author (not in a training position):
Dale L Bailey *PhD*
Department of Nuclear Medicine
Royal North Shore Hospital
St Leonards, NSW, Australia 2065
E: Dale.Bailey@sydney.edu.au
T: +61 (0)2 9926 4440
F: +61 (0)2 9926 4099

Running Title:

$^{64/67}$Cu-SARTATE Imaging & Therapy

Wordcount (total): 5356

Reference: JNUMED/2022/264586

ABSTRACT

Aim: To report the use of copper-64 and copper-67 as a theranostic pair of radionuclides in human subjects. In addition, to measure whole organ dosimetry of copper-64 and copper-67 attached to the somatostatin analogue Octreotate using the sarcophagine MeCOSAR chelator ("SARTATE") in subjects with somatostatin receptor-expressing lesions confined to the cranium, thereby permitting normal organ dosimetry for the remainder of the body. **Methods**: Pre-treatment PET imaging studies were performed up to 24 hours after injection of [^{64}Cu]Cu-SARTATE and normal organ dosimetry estimates were made using OLINDA/EXM. Subsequently the trial subjects with multifocal meningiomas were given therapeutic doses of [^{67}Cu]Cu-SARTATE and imaged over a number of days using SPECT/CT. **Results**: Five subjects were initially recruited and imaged using PET/CT prior to treatment. Three of the subjects were subsequently administered four cycles each of [^{67}Cu]Cu-SARTATE followed by multiple SPECT/CT imaging timepoints. No serious adverse events (SAEs) were observed and no adverse events led to withdrawal from the study or discontinuation from treatment. The mean Effective Dose estimated was 3.95×10^{-2} mSv/MBq for [^{64}Cu]Cu-SARTATE and 7.62×10^{-2} mSv/MBq for [^{67}Cu]Cu-SARTATE. The highest estimated organ dose was in spleen followed by kidneys, liver, adrenals and small intestine. The matched pairing was shown by PET and SPECT intra-subject imaging to have near identical targeting to tumours for guiding therapy, demonstrating a potentially accurate and precise theranostic product. **Conclusions**: Copper-64 and copper-67 show great promise as a theranostic pair of radionuclides. Further clinical studies will be required to examine the therapeutic dose required for [^{67}Cu]Cu-SARTATE for various indications. In addition, the ability to use predictive copper-64 based dosimetry for treatment planning with copper-67 should be further explored.

INTRODUCTION

Copper-64 and copper-67 have been proposed as a potentially ideal pair of theranostic radionuclides (*1*). Copper-64 (^{64}Cu) has a 12.7 h physical half-life and emits positrons (β^+) with a maximum energy of 0.65 MeV at 17% abundance making it suitable for imaging with positron emission tomography (PET). Copper-67 (^{67}Cu) decays by β^- emissions in the range of 0.18 - 0.58 MeV at 100% abundance and emits readily imageable gamma photons at 0.092 MeV (23%) and 0.185 MeV (49%) with a physical half-life of 61.8 h. As both radionuclides are elemental copper, the chemistry for chelating the imaging agent and the therapeutic compound are essentially identical. Copper-64 is made in a cyclotron and yields can be realised so that patient doses can be provided on a commercial scale. Copper-67 is produced by high energy X-rays from an electron accelerator via the ^{68}Zn(γ,p)^{67}Cu reaction (*2*). Moreover, the chelation chemistry of radio-copper is well developed (*1*). Given these recent chelation and production developments there is currently significant interest in the use of ^{64}Cu/^{67}Cu as a theranostic pair (recently termed "Targeted Copper Theranostic" or TCT).

The ^{64}Cu/^{67}Cu pairing offers significant advantages compared to other theranostic pairs such as ^{68}Ga/^{177}Lu including:

- the extended physical half-lives of both ^{64}Cu and ^{67}Cu permit centralised production and widespread transportation of ready-to-use theranostic agents for both diagnosis and therapy to remote sites which is generally not possible with generator-produced ^{68}Ga;
- Scalable product supply for ^{64}Cu and ^{67}Cu due to favourable production methods using cyclotrons and accelerators respectively;
- ^{64}Cu can be imaged on the day of administration (as with current PET radionuclides such as ^{68}Ga) but also offers the ability to collect images up to 48 hours after administration for flexible patient scheduling and potentially improved lesion identification;
- ^{67}Cu emits abundant gamma photons which are well suited for SPECT imaging as well as a β^- particle for therapy with a similar energy and path length in tissue to ^{177}Lu;
- ^{67}Cu ($t_{½}$ = 2.6 days) has a shorter half-life than ^{177}Lu ($t_{½}$ = 6.7 days), making it well matched to peptide pharmacokinetics presenting less of a radiation protection challenge and may allow more frequent administrations;
- the longer physical half-life of ^{64}Cu compared to ^{68}Ga improves ability for pre-therapy dosimetry estimates using PET imaging at multiple timepoints potentially leading to a personalised treatment approach.

In this paper we report the first-in-human use of copper-64 and copper-67 as a theranostic pair for treatment planning and therapy. The primary aims of the study were to assess safety, biodistribution and dosimetry of both copper radionuclides labelled to the somatostatin analogue Tyr^3-octreotate (H-D-Phe-Cys-Phe-D-Trp-Lys-Thr-Cys-Thr-OH) conjugated to the MeCOSAR sarcophagine chelator ("SARTATE") (*3*). The trial design was an open-label, non-randomised phase I safety study in adult subjects with meningiomas using fixed dosing of both the diagnostic and therapeutic investigational medical products, [^{64}Cu]Cu-SARTATE and [^{67}Cu]Cu-SARTATE respectively. [^{64}Cu]Cu-SARTATE binds to tumours expressing somatostatin receptors type 2 ($SSTR_2$) (*4*) which has been shown to be over-expressed in meningiomas (*5*). This subject population was selected for the study due to the high unmet clinical need and the expected normal uptake in organs outside of the calvarium thus permitting normal organ dosimetry measures, which is not the case with typical $SSTR_2$ expressing cancers in subjects with metastatic neuroendocrine tumours (NETs).

MATERIALS & METHODS

Production of Radionuclides of Copper

[^{64}Cu]$CuCl_2$ was manufactured on a biomedical cyclotron (PET Trace, GE Healthcare, Milwaukee, WI, USA) via the ^{64}Ni(p,n)^{64}Cu nuclear reaction, and a subsequent purification on an automated synthesizer (Comecer, Castel Bolognese RA, Italy) (*6*).

[^{67}Cu]$CuCl_2$ was obtained by irradiation of enriched ^{68}Zn targets at 40 MeV on a linear electron accelerator (Idaho Accelerator Center, Pocatello, Idaho, USA) via the reaction process ^{68}Zn(γ,p)^{67}Cu. After irradiation, Zn and Cu are separated by low pressure evaporation and subsequently purified using anion exchange column chromatography. Final product pH was adjusted to 2.0 (nominal) and volume activity of > 40 MBq/μL (~1mCi/μL). Typical specific activities were greater than 7 TBq/mg (~200 Ci/mg).

Subject Selection and Recruitment

The subjects enrolled in this trial all had unresectable, multifocal meningiomas that were progressing despite treatment with chemotherapy and radiotherapy. A consequence of the cranial localisation of the disease is that it enables assessment of the normal biodistribution in the visceral organs, with little prospect of the disease being present, or affecting biodistribution, to derive normal organ dosimetry. Previous studies using [^{64}Cu]Cu-SARTATE in humans (*4*) recruited subjects with neuroendocrine tumours

(NETs) where metastatic disease was often present throughout the abdomen and in organs such as liver and pancreas and thus estimation of normal organ dosimetry was not always possible. Using subjects with cranial lesions avoids this issue. The study (ClinicalTrials.gov Identifier: NCT03936426) was approved by a nationally accredited Human Research Ethics Committee (St Vincent's Hospital Melbourne HREC, Ref: HREC/17/SVHM/238) and signed written informed consent was obtained from all subjects prior to recruitment.

Imaging Studies

Prior to commencing the trial the quantitative accuracy of the PET scanner (Biograph mCT/64, Siemens Healthineers, Hoffman Estates, IL, USA) was validated with a modified version of the protocol developed by our national imaging clinical trials group (ARTnet – the Australasian Radiopharmaceutical Trials network) (*7*) adapted for ^{64}Cu PET imaging. The protocol used a NEMA NU-2 Image Quality phantom and demonstrated the mean SUV in the main compartment of the phantom to be accurate to within ±5% of the true value of 1.0 (*i.e.*, SUV = 0.95 – 1.05). ^{64}Cu used for the dose calibrator and camera validation was traceable to the primary Australian ^{64}Cu standard established by the national nuclear science body, the ANSTO Nuclear Metrology group (Australian Nuclear Science & Technology Organisation, Lucas Heights, NSW, Australia).

[^{64}Cu]Cu-SARTATE Preparation, Administration and Imaging

[^{64}Cu]Cu-SARTATE was prepared at a radiopharmaceutical manufacturing facility in Adelaide on Day -1 and transported by plane overnight to our centre in Sydney. There was no specific preparation required of the subjects and, in particular, no subjects were on any medication such as somatostatin analogues which could potentially interfere with uptake and biodistribution. The [^{64}Cu]Cu-SARTATE was administered on Day 0 as ~200 MBq delivered as a slow bolus intravenous injection. Imaging was acquired on the time-of-flight PET/CT system with a 21.6 cm axial field view in fully 3D acquisition mode at multiple timepoints after administration: 1 hour, 4 hours and 24 hours. On Day 0, scans were acquired for three minutes per bed position with coverage from the vertex of the skull to the mid-thigh. To partially compensate for radionuclide decay, on Day +1 the scan acquisition time was extended to 5 mins per bed position. Image reconstruction used CT-based scatter and attenuation correction, time-of-flight localisation, and a resolution recovery algorithm (TrueX™, Siemens Healthineers) followed by a post-reconstruction Gaussian 3D filter with FWHM of 5.0 mm.

[^{67}Cu]Cu-SARTATE Preparation, Administration and Imaging

[^{67}Cu]Cu-SARTATE was manufactured on site in our local hospital radiopharmacy facility using the imported copper-67. The trial protocol was designed so that a reliable, repeatable administration of a minimum of 5 GBq of [^{67}Cu]Cu-SARTATE was achievable.

Briefly, the [^{67}Cu]Cu-SARTATE was prepared manually by the reaction of [^{67}Cu]$CuCl_2$ in 0.1M HCl with SARTATE (60 μg, GMP grade, Auspep Clinical Peptides, Melbourne, Australia) according to previously optimised methods for production and quality control. The purity and safety of the product for release was assessed with radio-TLC, radio-HPLC, pH, pyrogenicity, sterile filter integrity and post-release sterility.

The subjects in this trial received the [^{67}Cu]Cu-SARTATE as a ramped, slow infusion over 20 minutes. All subjects had co-administration of one litre of amino acid solution (5.8 g lysine and 11.5 g arginine per litre) over 3-4 hours for renal protection commencing 30 minutes prior to the [^{67}Cu]Cu-SARTATE administration and regular clinical observations including ECGs performed from the time of administration. Subjects were asked to void their bladder before the injection and instructed not to void again until after the first scan at +1 hour, to allow a cross-check of the total radioactivity in the reconstructed images and comparison with the known amount of ^{67}Cu injected. All ^{67}Cu imaging was performed as whole-body SPECT/CT scans on a dual detector gamma camera (Intevo.6, Siemens Healthineers, Hoffman Estates, IL, USA), with a thicker scintillation detector (16 mm) than is standard for increased sensitivity for medium and higher energy photons such as from ^{67}Cu, from the vertex of the skull to the mid-thigh and subsequently reconstructed using in-house protocols and software to produce quantitative SPECT images (*8*). A calibration source (~125 mL) containing ~40 MBq ^{67}Cu was included in one bed position at each timepoint. The acquisition consisted of three contiguous bed positions each of approx. 38 cm in axial extent. Imaging was acquired on Days 0, +1 and +4 at the approx. timepoints of 1, 4, 24 and 96 hours post-administration. In addition, on Day +1, a 2D planar ANT/POST whole body "sweep" was acquired. Images were acquired using a medium energy collimator with the main PHA window over the 185 keV ± 10% photopeak and a lower energy scatter window (143 – 163 keV). All SPECT data were acquired using continuous detector rotation into 120 projections over 360° in a 128 × 128 matrix. The time per projection varied; for both acquisitions on Day 0 (1 h and 4 h post-infusion) it was 8 secs/projection, on Day +1 it was 10 secs/projection and on Day +4 it was 12 secs/projection. Images were reconstructed using the Ordered Subset Expectation Maximisation (OSEM) algorithm (*9*) after scatter correction in projection space using an in-house implementation of the Transmission-Dependent Scatter Correction method (*8,10*) on a

dedicated nuclear medicine workstation (HERMES Medical Ab, Stockholm, SWE) followed by a post-reconstruction attenuation correction based on the CT scan using a modified version of the method of Chang (*8,11*). Finally, the images were converted to units of kBq/cc for further analysis.

The complete set of data acquired for the [^{64}Cu]Cu-SARTATE PET prior to treatment and [^{67}Cu]Cu-SARTATE for each cycle provided three PET/CT scans and 16 (4 cycles $\times$ 4 time points per cycle) whole-body SPECT/CT scans per individual for analysis.

Biodistribution and Radiation Dosimetry

Both the PET and SPECT data were processed to determine organ biodistribution over time and whole-body radiation dosimetry. Organs-of-Interest were defined on the CT and functional (PET or SPECT) multimodality images at the baseline time point in each image series and transferred to the subsequent timepoints. [^{64}Cu]Cu-SARTATE and [^{67}Cu]Cu-SARTATE studies were considered separately. The ^{67}Cu calibration source in the field of view was checked for total radioactivity remaining to assess the accuracy of the quantitative SPECT images. Estimates of whole-body retention were also made based on the imaging with an adjustment for the missing lower limbs. Organs-of-Interest were defined for liver, spleen, kidneys, lungs, blood pool, L4-L5 lumbar spine (for bone marrow estimates), adrenal and parotid glands, urinary bladder and small bowel using a dedicated nuclear medicine workstation (MIM Encore™, MIM, Cleveland, OH, USA). Brain estimates of radioactivity were not included due to the presence of disease within the skull. The total uptake in each organ was calculated and converted to percentage of injected dose (%ID). The blood pool estimate was scaled by the blood volume based on the concentration of the radionuclide measured in the images and total blood volume in the models (male and female) used in the OLINDA/EXM program (*12*), based on standard MIRD adult models (*13*). A similar approach was used for thigh-based muscle VOI. The estimate of %ID in bone marrow was based on the L4-L5 vertebrae containing ~7% of the average total bone marrow in an adult (*14,15*). The corresponding Time-Activity Curve (TAC) data were imported into the OLINDA/EXM whole organ dosimetry package after decay correction with the respective half-lives for each radionuclide.

Dosimetry for [^{64}Cu]Cu-SARTATE and [^{67}Cu]Cu-SARTATE

All subjects who were selected to proceed to therapy had dosimetry estimates calculated for the PET imaging component of the trial. To allow direct comparison with the previously published dose estimates of a similar radiopharmaceutical, [^{64}Cu]DOTA-Octreotate (*16*), we employed a dynamic bladder model in

the OLINDA analysis based on an estimated urinary excretion fraction of 10% with a presumed 2 h voiding interval and a biological half-life of 1 h. The same assumptions and parameters used for the calculation of the radiation absorbed dose estimates for [^{64}Cu]Cu-SARTATE above were applied for the absorbed doses estimates from [^{67}Cu]Cu-SARTATE. All ^{67}Cu data were decay corrected prior to entry into OLINDA.

RESULTS

Subject Selection and Recruitment

Five subjects (four males, one female) were initially recruited to the trial of which three went on to receive the therapy. One of the subjects who did not proceed to therapy was precluded due to the post-recruitment disclosure of a previous malignancy (a skin lesion) and hence did not satisfy the inclusion criteria. The other subject who did not proceed on the trial to therapy was diverted to [^{177}Lu]Lu-DOTA-Octreotate treatment due to rapid disease progression and conflicts with the scheduling of the ^{67}Cu radionuclide. These two subjects who did not proceed to therapy were not included in the dosimetry calculations. All three remaining subjects (two males, one female) had unresectable, multi-focal meningiomas previously treated with radiotherapy and chemotherapy and no other malignancies. Table 1 shows the imaging data that were acquired for the three therapy subjects at all imaging time points.

Table 1. Imaging Data Acquired at the Various Time points in all Subjects

Approx. Time after Administration (h)	^{64}Cu PET	^{67}Cu Cycle 1 SPECT	^{67}Cu Cycle 2 SPECT	^{67}Cu Cycle 3 SPECT	^{67}Cu Cycle 4 SPECT
1	✓	✓	✓	✓	✓
4	✓	✓	✗ (2/3)	✓	✓
24	✓	✓	✓	✓	✓
96	N/A	✓	✓	✓	✓

✓Indicates all 3 subjects had all imaging at this timepoint. Only one timepoint in one subject was omitted (Subject B, Cycle 2, Day 0, +4 hours) due to a very delayed start of the infusion, precluding a measurement late in the evening.

Imaging Studies

[^{64}Cu]Cu-SARTATE Preparation, Administration and Imaging

The average amount of [^{64}Cu]Cu-SARTATE administered was 186 MBq (range: 176-207 MBq). No adverse events were recorded after the [^{64}Cu]Cu-SARTATE injection in any subject. An example set of images for one subject is shown in figure 1.

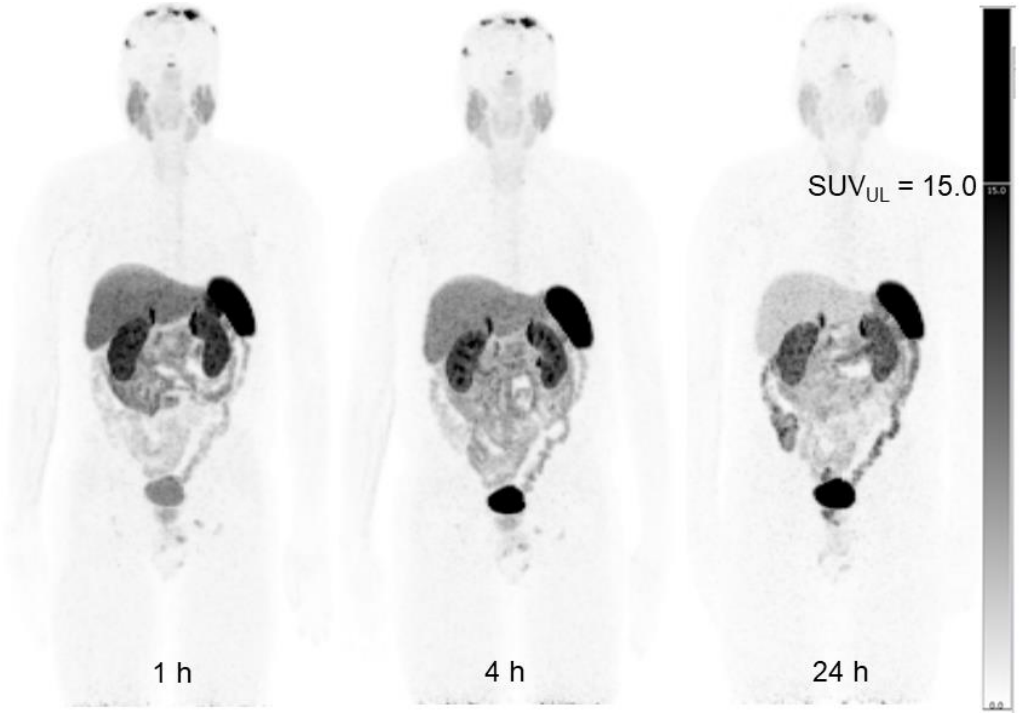

Figure 1. Example of the multiple timepoint maximum intensity projections (MIPs) with [^{64}Cu]Cu-SARTATE PET at 1, 4 and 24 h after injection. Considerable washout of the radiopharmaceutical is seen from liver, parotid glands and intracranial lesions at 24 hours. The grey scale is constant for all images with display range SUV = 0 – 15.

[^{67}Cu]Cu-SARTATE Preparation, Administration and Imaging

The amount of [^{67}Cu]Cu-SARTATE produced over the 12 cycles was 9660 ± 828 MBq and all batches were within specifications. The purity and safety of the product were measured by radio-TLC (average 98.9 ± 0.6 %), radio-HPLC (average 96.4 ± 2.8 %), pH (7.0), pyrogenicity (< 5.0 EU/mL), and sterile filter integrity and post-release sterility were confirmed.

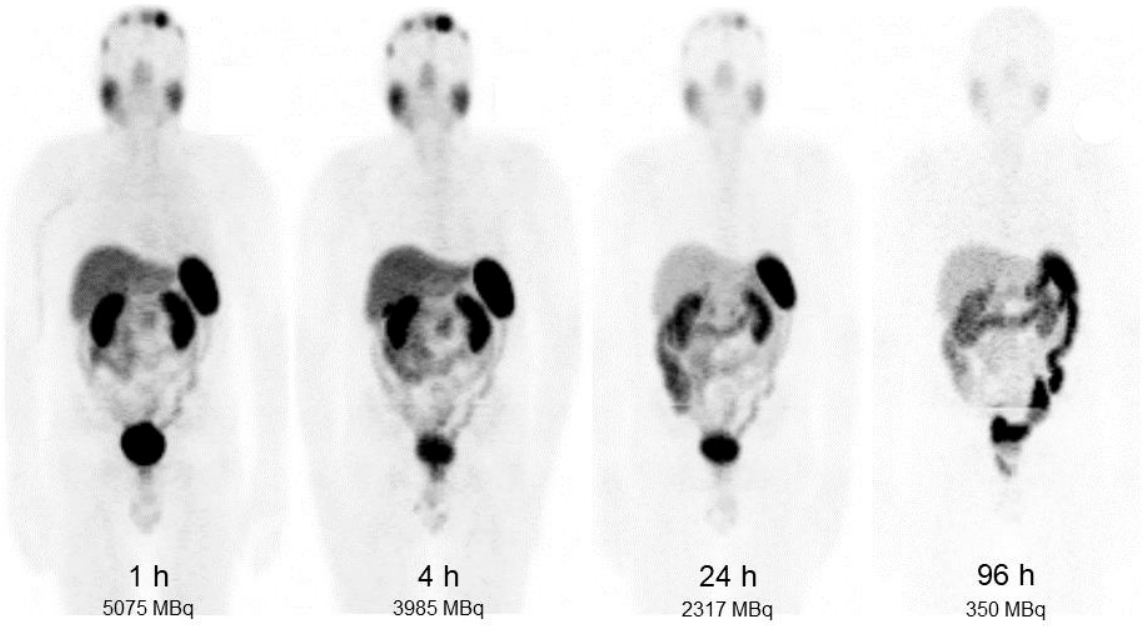

Figure 2. SPECT MIP images for the same subject as in Figure 1 are shown for each imaging timepoint in cycle 1 of treatment. Total radioactivity estimated in the subject is shown at each time point. The grey scale is not constant in this example due to the wide dynamic range and hence is not displayed. Good image quality with SPECT imaging was obtained up to the 96 h timepoint. The calibration standard was removed from the images before display.

The three subjects received an average of 4945 ± 100 MBq (range: 4695 – 5076 MBq) of [^{67}Cu]Cu-SARTATE over a combined total of 12 cycles of treatment. SPECT MIP images for the same subject as for figure 1 are shown in figure 2 with the additional timepoint (96 h) facilitated by the longer half-life of ^{67}Cu. Figure 3 shows a comparison of the uptake for both the [^{64}Cu]Cu-SARTATE and [^{67}Cu]Cu-SARTATE through the largest tumour in the subject.

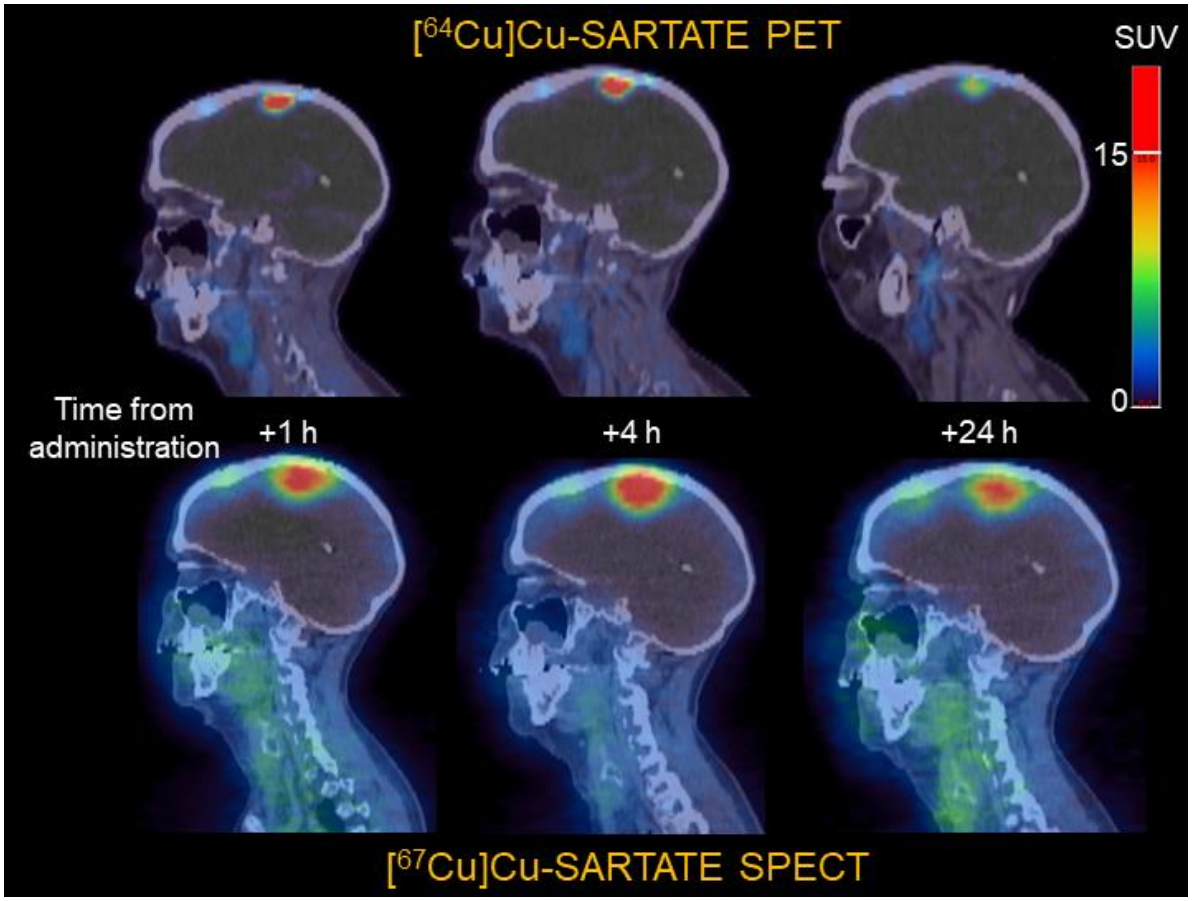

Figure 3. The reproducibility of the copper theranostic PET and SPECT pairing is shown in this comparison of SARTATE where targeting of the two compounds using PET and SPECT at equivalent time points after administration are shown. The change of radionuclide from copper-64 to copper-67 does not alter the targeting to the tumour in this subject. The SPECT images are from cycle 1 of treatment. The volume of the main lesion in the SPECT images appears greater than in the PET images due to the poorer spatial resolution of SPECT. The PET images are shown at a fixed SUV upper threshold (max = 15) while the SPECT images are shown with individual scaling. The 96 h SPECT time point has been omitted as there was no comparable PET image.

Safety, Biodistribution and Radiation Dosimetry

Adverse Events

Both [^{64}Cu]Cu-SARTATE and [^{67}Cu]Cu-SARTATE were safe and well-tolerated in all subjects. No serious adverse events (SAEs), no potentially life-threatening (Grade 4) treatment emergent adverse events (TEAEs) and no deaths were recorded during the study period. Further, there were no treatment discontinuations/interruptions and no withdrawals from the study due to TEAEs. There were no TEAEs considered related to [^{64}Cu]Cu-SARTATE administration. Sixteen TEAEs were considered due to [^{67}Cu]Cu-SARTATE which included decreased lymphocyte count (13 TEAEs) in the three therapy subjects. Further details of the adverse events are included in the online supplementary file (Supplementary Tables 1 and

2). There were no notable safety findings arising from review of the ECGs, vital signs and physical examination data.

Biodistribution Data

The decay-corrected radionuclide retention curves from the PET and SPECT imaging at all four cycles for each subject are shown in figure 4. It is seen that the whole-body retention is highly reproducible over all cycles of treatment. For the [^{67}Cu]Cu-SARTATE biodistribution, the organ that exhibited the highest total uptake expressed as percentage of injected dose (%ID) was liver followed by kidney, spleen and the lungs. The averaged biodistribution for all subjects and all cycles of treatment is shown in table 2 as the amount of the radiopharmaceutical in the organs at each time point. The individual subject biodistribution data for each cycle and each time point are included in the online supplementary file (Supplementary Tables 3-5).

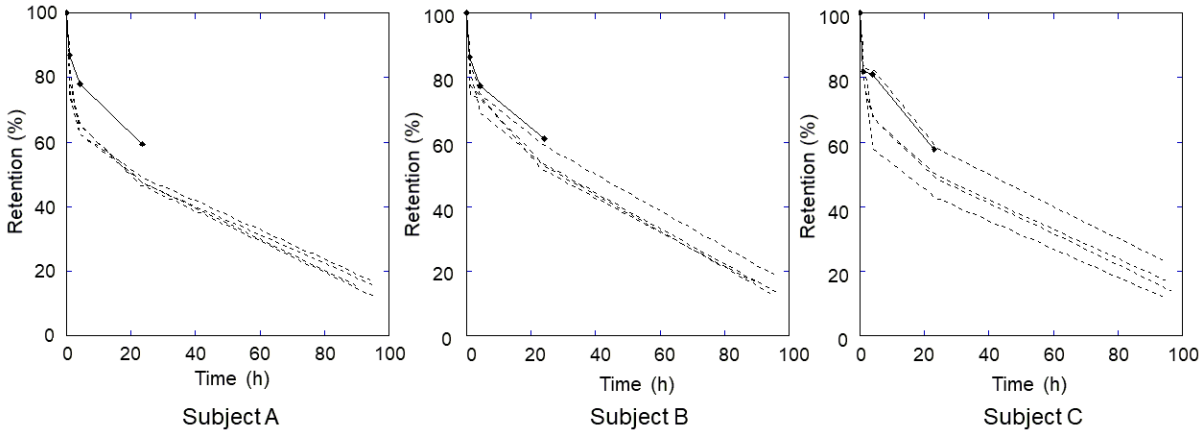

Figure 4. Whole body retention determined from the PET and SPECT imaging is shown for each subject. The PET retention of [^{64}Cu]Cu-SARTATE is shown as the solid line while the dashed lines are for each of the four cycles of [^{67}Cu]Cu-SARTATE measured out to approx. 96 hrs post-treatment. The curves are corrected for radionuclide decay and normalised to the amount of radiopharmaceutical administered (100%). The [^{64}Cu]Cu-SARTATE retention remains on the upper side of the [^{67}Cu]Cu-SARTATE retention curves in all cases, possibly reflecting the influence that the co-administered amino acid infusion on treatment day has on retention of [^{67}Cu]Cu-SARTATE.

Table 2. Average [^{67}Cu]Cu-SARTATE biodistribution data (percent injected dose (%ID) per organ) for all three subjects over all four treatment cycles (values corrected for radioactive decay) at each of the time points.

Scan time point	Time from IVI (hrs)	Adrenals (%ID)	Heart Cont. (%ID)	Liver (%ID)	Lungs (%ID)	Kidneys (%ID)	LLI (%ID)	Pancreas (%ID)	Red Marrow (%ID)	Sm Intest. (%ID)	Spleen (%ID)	Urin Bladder (%ID)	Remainder (%ID)	TOTAL (% ID)
1	1	0.05	0.39	8.7	2.8	4.5	0.47	1.23	1.6	2.2	2.8	5.6	69.6	100.0
2	4	0.05	0.26	8.6	2.3	4.1	0.38	0.91	1.5	2.3	3.1	1.3	63.2	88.0
3	24	0.04	0.19	4.4	1.5	3.0	0.51	0.53	1.2	1.7	2.4	1.5	47.9	64.9
4	96	0.02	0.02	1.9	0.5	1.1	0.21	0.04	0.4	0.6	0.7	0.6	14.7	20.7

KEY: Heart Cont. - Heart Contents, LLI – Lower Large Intestine, Sm.Intest. – Small Intestine, Urin.Bladder – Urinary Bladder, Remainder – all other radioactivity outside of the organs listed.

Dosimetry for [^{64}Cu]Cu-SARTATE and [^{67}Cu]Cu-SARTATE

The averaged radiation dosimetry estimates of [^{64}Cu]Cu-SARTATE for the PET & SPECT imaging components of the trial from the three subjects who proceeded to therapy are shown in table 3. The highest organ dose per MBq was in spleen followed by kidneys, liver, adrenals and small intestine. This was consistent for both [^{64}Cu]Cu-SARTATE and [^{67}Cu]Cu-SARTATE. The difference in dosimetry between the two SARTATE radiopharmaceuticals used averaged a factor of 2.6 (range: 1.3 – 4.0) with the copper-67 product conferring the higher dose, although this factor was not consistent between different organs. This may be due to altered biodistribution kinetics due to the use of the amino acid infusion when administering the therapeutic product, especially in the first four hours.

Table 3. Organ Absorbed Doses from [^{64}Cu]Cu-SARTATE and [^{67}Cu]Cu-SARTATE – mean of 3 subjects. The [^{67}Cu]Cu-SARTATE estimates are based on all four cycles estimated independently in each subject and then averaged across all three subjects. The mean Effective Dose for [^{64}Cu]Cu-SARTATE was 3.95×10^{-2} mSv/MBq and for[^{67}Cu]Cu-SARTATE it was 7.62×10^{-2} mSv/MBq.

Organ	[^{64}Cu]Cu-SARTATE Mean Absorbed Dose (mGy/MBq)	[^{67}Cu]Cu-SARTATE Mean Absorbed Dose (mGy/MBq)	Ratio of Dose (mGy) ^{67}Cu:^{64}Cu
Adrenals	8.30×10^{-2}	1.79×10^{-1}	2.2
Brain	1.29×10^{-2}	4.12×10^{-2}	3.2
Breasts	1.32×10^{-2}	3.85×10^{-2}	2.9
Gallbladder Wall	2.42×10^{-2}	5.43×10^{-2}	2.2
LLI Wall	3.68×10^{-2}	1.13×10^{-1}	3.1
Small Intestine	5.00×10^{-2}	1.58×10^{-1}	3.2
Stomach Wall	2.07×10^{-2}	4.88×10^{-2}	2.4
ULI Wall	2.00×10^{-2}	5.14×10^{-2}	2.6
Heart Wall	2.06×10^{-2}	5.42×10^{-2}	2.6
Kidneys	2.46×10^{-1}	5.45×10^{-2}	2.2
Liver	9.90×10^{-2}	1.73×10^{-1}	1.7
Lungs	3.85×10^{-2}	8.50×10^{-2}	2.2
Muscle	1.56×10^{-2}	2.54×10^{-2}	1.6
Ovaries	1.79×10^{-2}	4.85×10^{-2}	2.7
Pancreas	4.12×10^{-2}	7.98×10^{-2}	1.9
Red Marrow	2.11×10^{-2}	6.19×10^{-2}	2.9
Osteogenic Cells	3.22×10^{-2}	1.30×10^{-1}	4.0
Skin	1.20×10^{-2}	3.66×10^{-2}	3.0
Spleen	4.78×10^{-1}	6.42×10^{-1}	1.3
Testes	1.19×10^{-2}	4.08×10^{-2}	3.4
Thymus	1.46×10^{-2}	4.08×10^{-2}	2.8
Thyroid	1.35×10^{-2}	5.34×10^{-2}	3.9
Urinary Bladder Wall	3.81×10^{-2}	6.22×10^{-2}	1.6
Uterus	1.77×10^{-2}	5.23×10^{-2}	3.0
Total Body	2.32×10^{-2}	5.19×10^{-2}	2.2

DISCUSSION

The potential clinical use of the radionuclides of copper, predominantly ^{64}Cu and ^{67}Cu, was suggested over 40 years ago (*17*). Subsequently in 1995 Schwarz *et al* reported a pre-clinical study in rodents bearing lymphomas examining the radiation dosimetry from ^{64}Cu and ^{67}Cu radiolabelled [Cu]benzyl-TETA-1A3 monoclonal antibody (mAb) and reported a 5-fold increase in radiation absorbed dose per unit radioactivity for the longer-lived ^{67}Cu compared with ^{64}Cu (*18*). Subsequently, DeNardo *et al* reported the use of a ^{67}Cu radiolabelled mAb ([^{67}Cu]2IT-BAT-Lym-1) in subjects with Stage 3 or 4 B-cell lymphoma to

assess feasibility for subsequent treatment (*19,20*). Remarkably, while they only administered what they believed would be an amount of [^{67}Cu]2IT-BAT-Lym-1 which would be sufficient for their imaging and dosimetry studies they reported achieving good clinical responses in 7 out of the 11 subjects who displayed cutaneous lesions, achieving almost 50% average reduction in lesion size. Further studies by this group compared the therapeutic potential of ^{64}Cu and ^{67}Cu in a hamster model bearing human colon cancers and found that they were equivalent in this cell line and animal model (*21*). It is worth noting that while ^{64}Cu is primarily thought of as a positron (β^+) emitting radionuclide for PET imaging, the branching ratio for positrons is only 17% whereas it also emits beta-minus particles (β^-) with 39% abundance.

To the best of our knowledge the data reported in this work represent the first documented use of combined ^{64}Cu and ^{67}Cu as a clinical theranostic pair in humans. The pairing of ^{64}Cu with ^{67}Cu has been used to firstly confirm and localise tumour targeting in the subjects (with ^{64}Cu) and the subsequent delivery and retention of the therapeutic product (with ^{67}Cu). Almost identical diagnostic and therapeutic drug products were administered using the different radioisotopes of copper for each role which represents the ideal "same element" theranostic pairing. The use of "different element" theranostic pairs such as ^{68}Ga or ^{111}In for imaging paired with either ^{90}Y or ^{177}Lu for therapy, for example, has been shown to potentially alter the biodistribution of the product between imaging and therapy (*22*). Based on the imaging data in this paper there is a high level of confidence that the targeting seen in the PET study will truly reflect the therapeutic radiopharmaceutical delivery and retention, hence demonstrating a particularly attractive characteristic of the copper pairing (Figure 3).

Compared to conventional diagnostic imaging PET radionuclides (*e.g.*, ^{18}F, ^{68}Ga) which have physical half-lives of less than two hours the longer half-lives of the copper radionuclides used here have a number of advantages. One is that both SARTATE products can potentially be radiolabelled in a centralised, GMP-licenced facility and transported to the clinical centre for use. In our case, the [^{64}Cu]Cu-SARTATE product is manufactured in Adelaide, South Australia, and flown overnight to Sydney, NSW, a distance of approx. 1200 kms. Centralised manufacture obviates the need for the local PET facility to invest in expensive radiopharmaceutical synthesis equipment and staff required to perform the radiolabelling, production and QA of the PET radiopharmaceutical. The [^{67}Cu]Cu-SARTATE can be made in the same production facility and transported in an identical manner, however, for this early proof-of-principle trial we chose to perform the radiolabelling locally on site because the ^{67}Cu was produced in Idaho, USA and had to take a

number of flights to transport it 13,000 km to Sydney with the half-life of just over 60 hours being a consideration.

The Effective Dose of the most commonly used $SSTR_2$ targeting PET radiopharmaceutical, [^{68}Ga]Ga-DOTA-Octreotate, is 4.2 mSv for 200 MBq (*23*). The trial design used here was informed by previous preliminary dosimetry estimates using [^{64}Cu]Cu-SARTATE in subjects with neuroendocrine tumours (*4*) which reported whole body Effective Dose of 4.5×10^{-2} mSv/MBq or approx. 9mSv per 200 MBq. Previously, dose estimates in major organs for a different copper-64 labelled $SSTR_2$-tageting agent, [^{64}Cu]Cu-DOTA-Octreotate, have been published (*16*). The Effective Dose of [^{64}Cu]Cu-DOTA-Octreotate was reported to be 6.3 mSv for 200 MBq (*16*). The average Effective Dose measured in the three subjects in this trial with [^{64}Cu]Cu-SARTATE was 3.95×10^{-2} mSv/MBq, which equates to approx. 8 mSv for 200 MBq administered, similar to the value reported by Hicks *et al* (*4*) with the slight increase in the latter potentially reflecting that the subjects in their series had metastatic disease which may affect the estimates. In a PET/CT examination from vertex of skull to mid-thigh the X-ray CT contribution is an additional 8-15 mSv (*24*), so the estimated difference of ~4 mSv between [^{68}Ga]Ga-DOTA-Octreotate (4.2 mSv) and [^{64}Cu]Cu-SARTATE (8 mSv) may be deemed acceptable when considering the total dose for the overall combined PET/CT examination.

This manuscript does not include any estimates of the absorbed dose to the intracranial lesions that were the therapeutic targets in this trial, dose/response relationships nor efficacy. One reason for this is that the limited spatial resolution of SPECT with a medium energy collimator and current technology is such that the radioactivity contained in any mass or lesion less than approximately 50 mm in cross-sectional dimension will be underestimated (*25*). New approaches to image reconstruction and post-processing are attempting to address this limitation (*26*). Most of the organs measured in this study are larger in size than the intracranial lesions and hence not subject to the same magnitude of underestimation. With the limited number of subjects that were enrolled (N=3) it was felt that dose/response and efficacy, which were secondary endpoints of the trial, would not be reliable to report and larger series would be required. Currently lesion dosimetry in the multifocal, metastatic setting remains time-consuming but could be improved with new machine-based learning approaches. We have not included [^{64}Cu]Cu-SARTATE estimated dosimetry for the [^{67}Cu]Cu-SARTATE treatment due to the differences in the physiological conditions under which the respective radiopharmaceuticals were administered (with and without amino acid infusion) and differences in the imaging technologies due to the large difference in spatial resolution

leading to potential underestimation of the SPECT-based image radiopharmaceutical concentrations in organs and other tissues (*27*) – see, for example, a comparison of the lesion sizes in PET and SPECT in figure 3. This is the subject of further ongoing investigation.

CONCLUSIONS

To the best of our knowledge this is the first reported use of [^{64}Cu]Cu-SARTATE and [^{67}Cu]Cu-SARTATE as a theranostic pair. Both compounds were shown to be safe and able to be studied over prolonged imaging time points. Both [^{64}Cu]Cu-SARTATE and [^{67}Cu]Cu-SARTATE were safe and well tolerated. No life-threatening or serious adverse events were observed nor any adverse events leading to withdrawal from the study or discontinuation of treatment. The matched pairing was shown by PET and SPECT imaging to have identical targeting to tumours for guiding therapy, demonstrating a near ideal theranostic product pair. The extended half-life and suitable PET imaging characteristics of copper-64 should allow for personalised dosimetry to be performed prior to treatment which is not possible at present with conventional PET imaging radionuclides such as ^{18}F and ^{68}Ga. Further studies will be required to examine the factors influencing the relationship between copper-64 estimated dosimetry and that observed after therapy with copper-67.

ACKNOWLEDGEMENTS

Harry Marquis was funded by a doctoral scholarship from the Sydney Vital Translational Cancer Research Centre (Cancer Institute NSW) and has received Travel Grant support from Sydney Vital. We are grateful to Clarity Pharmaceuticals (Sydney, Australia) for supplying the [^{64}Cu]Cu-SARTATE and [^{67}Cu]Cu-SARTATE used in this clinical trial.

CONFLICTS OF INTEREST

MH, CB and MP are employees and stockholders of Clarity Pharmaceuticals, the sponsor of this study. DLB has previously served as a member of the Clarity Pharmaceuticals Scientific Advisory Board. No other conflicts of interest relevant to this work exist.

SUMMARY

QUESTION: How do the radiation dosimetry estimates for Copper-labelled radiopharmaceuticals compare with conventional PET radiotracers?

PERTINENT FINDINGS: This study has demonstrated in three individuals that radiation dosimetry from copper-labelled radiopharmaceuticals is comparable to other widely used PET radiotracers such as FDG and Ga-68 labelled peptides and that copper-64 and copper-67 are a suitable theranostic pair of radionuclides.

IMPLICATIONS FOR PATIENT CARE: Copper-labelled radiopharmaceuticals are safe to use in diagnostic imaging and for radionuclide therapy. In addition, due to the longer physical half-lives these radiopharmaceuticals can be manufactured in a central radiopharmacy and transported large distances to the PET scanner facility which will provide greater access and convenience for patients.

REFERENCES

1. Blower PJ, Lewis JS, Zweit J. Copper radionuclides and radiopharmaceuticals in nuclear medicine. *Nucl Med Biol.* 1996;23:957-980.
2. Yagi M, Kondo K. Preparation of carrier-free ^{67}Cu by the ^{68}Zn(γ,p) reaction. *Intl J Appl Radiat Isot.* 1978;29:757-759.
3. Paterson BM, Roselt P, Denoyer D, et al. PET imaging of tumours with a ^{64}Cu labeled macrobicyclic cage amine ligand tethered to Tyr^3-octreotate. *Dalton Trans.* 2014;43:1386-1396.
4. Hicks RJ, Jackson P, Kong G, et al. ^{64}Cu-SARTATE PET Imaging of Patients with Neuroendocrine Tumors Demonstrates High Tumor Uptake and Retention, Potentially Allowing Prospective Dosimetry for Peptide Receptor Radionuclide Therapy. *J Nucl Med.* 2019;60:777-785.
5. Dutour A, Kumar U, Panetta R, et al. Expression of somatostatin receptor subtypes in human brain tumors. *Int J Cancer.* 1998;76:620-627.
6. Malinconico M, Boschi F, Asp J, et al. Automated production of Cu-64, Zr-89, Ga-68, Ti-45, I-123 and I-124 with a medical cyclotron, using a commercial solid target system. *Nucl Med Biol.* 2019;72:S6.
7. Francis R, Bailey DL, Hofman MS, Scott A. The Australasian Radiopharmaceutical Trials Network (ARTnet) - Clinical Trials, Evidence and Opportunity. *J Nucl Med.* 2020;62:755-756.
8. Willowson K, Bailey DL, Baldock C. Quantitative SPECT Reconstruction Using CT-Derived Corrections. *Phys Med Biol.* 2008;53:3099-3112.
9. Hudson HM, Larkin RS. Accelerated image reconstruction using ordered subsets of projection data. *IEEE Trans Med Imag.* 1994;MI-13:601-609.
10. Meikle SR, Hutton BF, Bailey DL. A transmission dependent method for scatter correction in SPECT. *J Nucl Med.* 1994;35:360-367.
11. Chang LT. A method for attenuation correction in radionuclide computed tomography. *IEEE Trans Nucl Sci.* 1978;NS-25:638-643.
12. Stabin MG, Sparks RB, Crowe E. OLINDA/EXM: the second-generation personal computer software for internal dose assessment in nuclear medicine. *J Nucl Med.* 2005;46:1023-1027.
13. Watson EE, Stabin MG, Siegel JA. MIRD formulation. *Med Phys.* 1993;20:511-514.
14. Cristy M. Active bone marrow distribution as a function of age in humans. *Phys Med Biol.* 1981;26:389-400.
15. Stabin MG. *Fundamentals of Nuclear Medicine Dosimetry*: p.151. Springer; 2008.
16. Pfeifer A, Knigge U, Mortensen J, et al. Clinical PET of Neuroendocrine Tumors Using ^{64}Cu-DOTATATE: First-in-Humans Study. *J Nucl Med.* 2012;53:1207-1215.
17. Apelgot S, Coppey J, Gaudemer A, et al. Similar lethal effect in mammalian cells for two radioisotopes of copper with different decay schemes, ^{64}Cu and ^{67}Cu. *Int J Radiat Biol.* 1989;55:365-384.
18. Schwarz SW, Cutler PD, Eichling J, I. Tumor dosimetry for Cu-64 and Cu-67-labeled Mab 1A3 for radioimmunotherapy. *J Nucl Med.* 1995;36:42 *(Abstract)*.
19. DeNardo SJ, DeNardo GL, Kukis DL, et al. ^{67}Cu-21T-BAT-Lym-1 Pharmacokinetics, Radiation Dosimetry, Toxicity and Tumor Regression in Patients with Lymphoma. *J Nucl Med.* 1999;40:302-310.
20. DeNardo GL, Kukis DL, Shen S, DeNardo DA, Meares CF, DeNardo SJ. ^{67}Cu-versus ^{131}I-labeled Lym-1 antibody: comparative pharmacokinetics and dosimetry in patients with non-Hodgkin's lymphoma. *Clin Cancer Res.* 1999;5:533-541.
21. Connett JM, Anderson CJ, Guo LW, et al. Radioimmunotherapy with a ^{64}Cu-labeled monoclonal antibody: a comparison with ^{67}Cu. *Proc Natl Acad Sci U S A.* 1996;93:6814-6818.
22. Miller C, Rousseau J, Ramogida CF, Celler A, Rahmim A, Uribe CF. Implications of physics, chemistry and biology for dosimetry calculations using theranostic pairs. *Theranostics.* 2022;12:232-259.
23. Walker RC, Smith GT, Liu E, Moore B, Clanton J, Stabin M. Measured human dosimetry of ^{68}Ga-DOTATATE. *J Nucl Med.* 2013;54:855-860.
24. Willowson KP, Bailey EA, Bailey DL. A retrospective evaluation of radiation dose associated with low dose FDG protocols in whole-body PET/CT. *Australas Phys Eng Sci Med.* 2012;35:49-53.
25. Ryu H, Meikle SR, Willowson KP, Eslick EM, Bailey DL. Performance evaluation of quantitative SPECT/CT using NEMA NU 2 PET methodology. *Phys Med Biol.* 2019;64:145017.

26. Marquis H, Deidda D, Gillman A, et al. Theranostic SPECT reconstruction for improved resolution: application to radionuclide therapy dosimetry. *Eur J Nucl Med Mol Imag Physics.* 2021;8:16.
27. Marquis H, Willowson KP, Bailey DL. Partial Volume Effect in SPECT & PET Imaging and Impact on Radionuclide Dosimetry Estimates. *Asia Ocean J Nucl Med Biol.* 2022;11(1) doi: 10.22038/ AOJNMB.2022.63827.1448.

Supplementary Data

Supplementary Table 1. [^{67}Cu]Cu-SARTATE related TEAEs by Preferred Term

Grade 1 (Mild)		Grade 2 (Moderate)		Grade 3 (Severe)	
Subject	**Preferred Term**	**Subject**	**Preferred Term**	**Subject**	**Preferred Term**
Relatedness to ^{67}Cu-SARTATE: DEFINITE					
B	Lymphocyte count decreased	B	Lymphocyte count decreased		
C	Lymphocyte count decreased	C	Lymphocyte count decreased		
Relatedness to ^{67}Cu-SARTATE: PROBABLE					
A	Lymphocyte count decreased	A	Lymphocyte count decreased	A	Lymphocyte count decreased
C	Lymphocyte count decreased	A	Lymphocyte count decreased		
C	Lymphocyte count decreased	C	Lymphocyte count decreased		
		C	Lymphocyte count decreased		
		C	Lymphocyte count decreased		
Relatedness to ^{67}Cu-SARTATE: POSSIBLE					
A	Oral herpes				
C	Tachycardia				
C	Dysgeusia				

Supplementary Table 2. [^{67}Cu]Cu-SARTATE related TEAEs by Common Terminology Criteria Grade

Preferred Term	Total Number of Events	Number of Grade 1 (Mild) Events*	Number of Grade 2 (Moderate) Events*	Number of Grade 3 (Severe) Events*	Number of Grade 4 (Life-threatening) Events*
Low lymphocytes	13	5	7	1	0
Oral herpes	1	1	0	0	0
Tachycardia	1	1	0	0	0
Dysgeusia	1	1	0	0	0

* Based on NCI Common Terminology Criteria for Adverse Events (CTCAE) Version 4.0.

Supplementary Table 3. Percentage injected dose (%ID) of [^{67}Cu]Cu-SARTATE in Subject A for all treatment cycles is shown in all measured organs and tissues. Data are decay-corrected for physical half-life.

Scan time point	Time from IVI (hrs)	Adrenals	Heart Cont.	Liver	Lungs	Kidneys	LLI	Muscle	Pancreas	Red Marrow	Sm Intest.	Spleen	Urin Bladder	Remainder
C1														
1	1.1	0.026	0.38	12.6	2.1	4.3	0.76	13.8	0.0	1.1	2.4	1.03	6.56	54.8
2	3.9	0.031	0.24	12.6	1.7	3.5	0.46	15.0	0.1	0.3	1.2	1.17	1.48	47.6
3	23.1	0.027	0.10	7.2	1.0	3.2	0.24	6.3	0.0	0.3	2.0	0.96	1.22	41.2
4	96.2	0.013	0.00	2.4	0.1	1.1	0.18	0.0	0.0	0.1	0.4	0.32	0.28	15.5
C2														
1	1.4	0.063	0.33	10.4	2.3	4.1	0.14	16.3	0.0	1.1	2.8	0.86	8.24	53.4
2	4.0	0.061	0.19	10.0	1.9	3.8	0.17	13.6	0.1	1.1	3.7	0.90	1.14	43.3
3	23.3	0.047	0.13	5.6	1.1	3.0	0.28	8.7	0.1	0.8	2.2	0.75	1.32	36.2
4	90.8	0.015	0.01	2.1	0.2	1.0	0.18	0.1	0.0	0.3	0.7	0.27	0.44	12.9
C3														
1	1.3	0.045	0.28	12.4	1.9	4.1	0.31	16.2	0.2	1.4	2.2	0.95	3.38	56.6
2	4.0	0.041	0.18	12.0	1.4	3.6	0.37	12.0	0.2	1.1	3.7	0.90	0.93	52.1
3	24.1	0.031	0.12	6.2	1.0	3.1	0.28	10.4	0.2	0.9	2.1	0.74	1.10	38.9
4	95.6	0.015	0.00	2.3	0.1	1.1	0.21	0.1	0.1	0.3	1.0	0.27	0.43	14.4
C4														
1	1.3	0.028	0.34	11.1	2.7	4.4	0.20	16.9	0.1	1.4	1.2	0.65	3.65	57.2
2	4.1	0.030	0.21	10.5	2.1	3.8	0.17	5.9	0.1	1.4	1.0	0.70	0.64	60.0
3	24.0	0.018	0.14	6.1	1.3	3.0	0.20	8.2	0.1	0.8	1.1	0.53	0.98	44.0
4	95.0	0.007	0.01	2.2	1.3	1.2	0.23	0.2	0.1	0.4	0.3	0.18	0.59	15.8
MEAN ALL CYCLES														
1	1.3	0.040	0.33	11.6	2.3	4.2	0.35	15.8	0.1	1.3	2.1	0.87	5.46	55.5
2	4.0	0.041	0.21	11.3	1.8	3.7	0.29	11.6	0.1	1.0	2.4	0.92	1.05	50.7
3	23.6	0.031	0.13	6.3	1.1	3.1	0.25	8.4	0.1	0.7	1.8	0.75	1.16	40.1
4	94.4	0.012	0.00	2.3	0.4	1.1	0.20	0.1	0.1	0.3	0.6	0.26	0.44	14.6

Supplementary Table 4. Percentage injected dose (%ID) of [^{67}Cu]Cu-SARTATE in Subject B for all treatment cycles is shown in all measured organs and tissues. Data are decay-corrected for physical half-life.

Scan time point	Time from IVI (hrs)	Adrenals	Heart Cont.	Liver	Lungs	Kidneys	LLI	Muscle	Pancreas	Red Marrow	Sm Intest.	Spleen	Urin Bladder	Remainder
C1														
1	1.0	0.018	0.41	8.8	3.2	4.3	0.26	3.7	0.04	2.3	1.7	5.5	2.5	67.3
2	3.9	0.018	0.29	8.5	2.5	3.6	0.19	5.6	0.03	2.2	1.7	6.0	1.3	57.5
3	22.7	0.014	0.22	4.4	1.8	2.7	0.24	4.3	0.03	1.7	1.3	4.5	2.6	47.6
4	94.9	0.006	0.04	2.5	0.4	0.8	0.08	0.2	0.01	0.0	0.4	1.3	0.3	21.2
C2														
1	1.3	0.022	0.33	7.1	3.1	3.8	0.19	7.3	0.03	2.0	1.1	4.0	2.1	68.9
2	-	-	-	-	-	-	-	-	-	-	-	-	-	-
3	23.0	0.023	0.22	3.3	1.8	2.5	0.09	4.7	0.03	1.8	1.0	3.2	0.8	48.4
4	90.4	0.011	0.04	1.5	0.4	0.9	0.02	0.8	0.01	0.6	0.1	0.8	1.1	14.7
C3														
1	1.5	0.043	0.35	7.9	3.9	4.0	0.17	7.7	0.12	2.3	2.0	4.0	1.2	66.3
2	4.0	0.047	0.19	7.4	3.4	3.2	0.14	6.9	0.11	2.0	2.5	4.2	1.4	67.3
3	23.1	0.036	0.32	4.3	2.6	2.8	0.11	4.8	0.11	2.1	1.8	3.3	1.1	49.2
4	95.9	0.015	0.02	1.9	0.6	0.8	0.23	0.4	0.04	0.5	0.4	0.8	0.3	12.6
C4														
1	1.4	0.058	0.33	8.5	3.0	3.8	0.20	9.3	0.10	2.5	1.0	4.3	4.3	62.6
2	4.1	0.045	0.28	8.3	2.5	3.2	0.17	8.6	0.06	2.2	0.7	4.2	1.2	54.4
3	24.4	0.034	0.26	4.4	1.9	3.0	0.14	6.2	0.09	1.8	0.5	3.2	1.3	43.7
4	94.3	0.016	0.03	2.0	0.5	1.0	0.01	0.2	0.03	0.7	0.1	0.8	0.2	11.0
MEAN ALL CYCLES														
1	1.3	0.036	0.36	8.1	3.3	4.0	0.21	7.0	0.07	2.2	1.5	4.5	2.5	66.3
2	4.0	0.037	0.25	8.1	2.8	3.4	0.17	7.1	0.07	2.1	1.6	4.8	1.3	59.7
3	23.3	0.027	0.25	4.1	2.0	2.7	0.14	5.0	0.06	1.9	1.1	3.5	1.4	47.2
4	93.9	0.012	0.03	2.0	0.5	0.9	0.08	0.4	0.02	0.4	0.3	0.9	0.5	14.9

Supplementary Table 5. Percentage injected dose (%ID) of [^{67}Cu]Cu-SARTATE in Subject C for all treatment cycles is shown in all measured organs and tissues. Data are decay-corrected for physical half-life.

Scan time point	Time from IVI (hrs)	Adrenals	Heart Cont.	Liver	Lungs	Kidneys	LLI	Muscle	Pancreas	Red Marrow	Sm Intest.	Spleen	Urin Bladder	Remainder
C1														
1	1.2	0.051	0.49	8.4	2.3	3.9	0.45	14.7	0.0	1.8	2.1	3.69	6.4	55.7
2	3.9	0.043	0.30	8.0	1.4	3.4	0.33	14.0	0.1	1.7	2.3	4.08	1.6	44.1
3	24.3	0.033	0.15	3.6	1.0	2.6	1.58	9.7	0.0	0.9	1.4	3.36	2.1	32.9
4	95.9	0.014	0.02	1.7	0.2	1.2	0.40	1.5	0.0	0.2	0.6	1.00	1.0	12.2
C2														
1	1.7	0.036	0.42	0.4	3.4	8.6	2.33	4.1	13.6	0.1	1.8	4.00	3.3	58.0
2	4.3	0.033	0.27	0.4	4.0	8.4	1.69	3.8	9.7	0.1	1.6	4.24	1.3	52.2
3	23.9	0.027	0.17	0.4	2.0	3.1	1.29	2.6	5.2	0.1	1.1	3.00	2.3	41.9
4	96.3	0.017	0.01	0.7	1.0	1.3	0.28	1.3	0.0	0.3	0.3	0.85	0.6	11.8
C3														
1	1.4	0.050	0.48	8.6	3.1	4.6	0.39	15.0	0.1	2.0	3.5	2.89	11.8	47.5
2	4.1	0.045	0.27	8.0	2.1	3.7	0.37	15.0	0.1	1.7	2.9	2.92	1.5	35.2
3	23.9	0.041	0.18	3.2	1.5	3.0	0.29	5.6	0.1	1.0	1.9	2.45	2.1	31.8
4	95.2	0.021	0.01	1.3	0.4	1.2	0.23	0.0	0.0	0.3	0.5	0.62	0.7	8.9
C4														
1	1.3	0.112	0.49	8.3	2.4	4.6	0.18	21.5	0.3	1.6	4.6	2.23	13.1	40.6
2	4.4	0.166	0.38	9.9	2.0	5.2	0.30	27.7	0.4	2.5	5.5	3.65	1.5	40.4
3	24.6	0.114	0.26	4.2	1.3	4.1	1.37	16.6	0.3	1.8	4.6	2.93	1.3	30.5
4	94.3	0.060	0.06	1.7	0.5	1.8	0.50	0.7	0.1	0.5	2.9	0.60	1.4	19.8
MEAN ALL CYCLES														
1	1.4	0.062	0.47	6.4	2.8	5.4	0.84	13.8	3.5	1.4	3.0	3.20	8.7	50.4
2	4.2	0.072	0.31	6.6	2.4	5.2	0.67	15.1	2.6	1.5	3.1	3.73	1.5	43.0
3	24.2	0.054	0.19	2.8	1.4	3.2	1.13	8.6	1.4	0.9	2.3	2.93	2.0	34.3
4	95.4	0.028	0.03	1.3	0.5	1.4	0.35	0.9	0.1	0.4	1.0	0.77	0.9	13.2